Inter-relationship between mean-daily irradiation and temperature, and decomposition models for hourly irradiation and temperature

E.J. Gago[1], **S. Etxebarria**[2], **Y. Tham**[2], **Y. Aldali**[2] **and T. Muneer**[2*]
[1]*Department of Civil Engineering, University of Granada, Spain;* [2]*School of Engineering and the Built Environment, Edinburgh Napier University, UK*

Abstract

Terrestrial temperature records have existed for centuries. These records are available for very many locations. Temperature is indeed the most widely measured meteorological parameter. In contrast, solar radiation being a parameter of secondary importance and also in view of the excessive measurement cost and the associated due care, it is recorded very infrequently. This article presents evaluation of a new type of model for mean-daily and hourly solar radiation based on temperature. The proposed model is of a very simple constitution and does not require any secondary meteorological parameters as required by other group of models that are available in literature. Furthermore, hourly temperature models are also presented that only require mean-daily temperature data. A comparison was undertaken regarding the performance of the presently proposed and previous models. It was found that the present models are able to provide reliable irradiation and hourly temperature estimates with a good accuracy.

Keywords: solar radiation; solar energy; solar radiation regression models

*Corresponding author.
t.muneer@napier.ac.uk

Received 21 July 2010; revised 25 August 2010; accepted 6 September 2010

1 INTRODUCTION

Solar radiation and daylight are essential to life on the earth. Solar radiation affects the earth's weather processes which determine the natural environment. Its presence at the earth's surface is necessary for the provision of food for mankind. Thus it is important to be able to understand the physics of solar radiation and in particular to determine the amount of energy intercepted by the earth's surface. The understanding of the climatological study of radiation is however comparatively new. Until 2010, there were only three stations in north-west Europe with irradiation records exceeding an 85-year period. In the UK, it was only in the 1950s that the Meteorological Office installed Kipp solarimeters. In contrast, however, temperature has been recorded the world over at very many locations and for a much longer period, e.g. the oldest records for temperature for Central England have existed since 1659! In India, to give another example, the number of sites with temperature records is 161, but only 18 stations measure irradiation. Likewise, respectively, in Malaysia and Spain, there exist 41 and 113 stations that measure temperature, but only 9 and 33 stations record irradiation. Table 1 provides information on the start dates for temperature records for England.

It has also been pointed out by Thornton and Running [1] and Rivisgton *et al.* [2] that even in the most developed countries such as the USA and Britain, the landmass area covered by solar radiation network is <1%. Globally this figure is much worse.

Solar irradiation availability of arbitrary surfaces is a prerequisite in many sciences. For example, agricultural meteorology, photobiology, animal husbandry, daylighting, comfort air-conditioning, building sciences and solar energy utilization all require this information. In agricultural meteorology, the importance of net radiation in determining crop evaporation is well documented. It has been suggested that the annual enthalpy of evaporation from short grass is equal to the annual net radiation. A similar case occurs on a daily basis. Net radiation is also required in estimating the heating coefficient of a field, which is a key index for soil germination temperature. The effects of solar radiation are also of interest in the breeding of cattle and other livestock. It is usually the major factor limiting the distribution of stock in the tropics. The heat load on

doi:10.1093/ijlct/ctq039 Advance Access Publication 6 October 2010

Table 1. *Start dates for temperature measurement for Central England.*

Year	Parameter recorded
1659	Monthly mean temperature
1772	Daily mean temperature
1878	Daily and monthly mean, maximum and minimum temperature

Table 2. *Monthly mean solar radiation and temperature for Madrid (40.38°N, 3.78°W).*

Month	Air temperature (°C)	Daily solar radiation: horizontal (kW h/m^2/day)
January	2.4	2.03
February	4.0	2.96
March	7.9	4.29
April	10.7	5.11
May	15.8	5.95
June	21.6	7.09
July	24.8	7.20
August	24.0	6.34
September	19.3	4.87
October	13.3	3.13
November	7.1	2.13
December	3.6	1.70

Source: http://eosweb.larc.nasa.gov/cgi-bin/sse/retscreen.cgi?email=rets@nrcan.gc.ca.

an animal is the result of solar irradiation and in some cases, its magnitude could be several times the animal's normal heat production. For most of the above applications, monthly averaged or daily solar radiation data are adequate.

The worldwide use of energy is rising by 2.5% a year, most of which is attributable to the accelerated consumption in the developed and now developing countries. It has been estimated that from a sustainability viewpoint, the developed countries will have to cut their use of energy by a factor of 10 within a generation. Proponents of solar energy have gone to the extent that they are calling for a complete substitution of conventional sources of energy with renewables. Their thesis is that the use of fossil fuels for energy production, even in minor quantities would merely postpone the collapse of the global environment.

The past three decades have seen a boom in the construction of energy efficient buildings which use solar architectural features to maximize the exploitation of daylight, solar heat, solar-driven ventilation and solar PV electricity. These applications require hourly solar radiation and temperature data.

In most areas of the world, especially in the developing countries, solar radiation measurements are not easily available due to the excessive cost and effort that is involved. Air temperatures, on the contrary, are routinely measured at most meteorological stations. As will be shown in Section 2, NASA provides a useful resource in terms of satellite-observed data for monthly irradiation and temperature. There is, however, a need to break down the daily data into the respective hourly components, as there is a significant swing of hourly temperature within any given day.

Table 3. *Sample of the TUTIEMPO data set for Madrid (40.38°N, 3.78°W) for May 2010.*

Day	T_{mean}	T_{max}	T_{min}
1	17.8	23.2	12.0
2	17.5	23.3	10.0
3	11.1	15.7	8.0
4	9.1	13.5	3.0
5	10.8	17.4	1.0
6	12.5	18.3	2.0
7	12.6	19.3	7.0
8	11.9	17.0	7.0
9	13.4	17.0	10.0
10	12.9	17.0	9.0
11	12.7	17.4	6.4
12	11.7	16.6	9.0
13	9.3	14.4	6.0
14	9.9	14.0	4.5
15	11.4	16.8	5.6
16	14.7	21.3	5.8
17	18.0	25.2	6.8
18	20.7	27.5	10.5
19	22.0	28.2	11.6
20	20.0	26.4	12.0
21	22.4	28.6	13.0
22	23.4	29.7	14.5
23	23.1	29.7	15.0
24	22.1	28.6	15.0
25	19.3	24.4	14.6
26	19.6	24.3	13.0
27	19.8	24.0	13.5
28	18.1	23.0	12.4
29	21.3	27.3	11.0
30	25.0	30.5	14.0
31	26.5	34.0	16.0

Source: www.TuTiempo.net.

The initial research related to solar radiation carried out by Angstrom [3] and others was concerned with the relationship between irradiation and the sunshine duration. Since then research in this field has come a long way. Today, a considerable amount of information is available on mathematical models that relate solar radiation to other meteorological parameters such as temperature, cloud-cover, rain amount, humidity and even visibility. However, as pointed out above, the parameter that has the largest measurement network is the ambient temperature. The aim of this work is to investigate the inter-relationship between:

- mean-daily solar radiation and mean, maximum and minimum temperature;
- daily mean, maximum and minimum temperature; and
- hourly temperature and the corresponding mean-daily maximum and minimum temperature.

2 PRESENTLY AVAILABLE INFORMATION

There are two reliable sources that provide information on the two of the most basic meteorological parameters: monthly mean temperature and solar radiation. These sources are the NASA website http://eosweb.larc.nasa.gov/cgi-bin/sse/retscreen.cgi?email=rets@nrcan.gc.ca and TUTIEMPO that is maintained by http://www.tutiempo.net/en/. NASA has produced a grid map of the world with information available for any given latitude and longitude. The solar radiation data are an estimate that has been produced from satellite-based scans of terrestrial cloud-cover. Typical tabulated information that may be downloaded from this source is shown in Table 2. Note that NASA does not provide the mean-daily maximum and minimum temperature. TUTIEMPO on the other hand provides daily mean, maximum and minimum temperature data for any given location. The data are based on measurements carried out by a wide network of meteorological stations and hence these latter data are more reliable. One of the subtasks of this work is also to check the reliability of the NASA temperature records by comparing them against the TUTIEMPO set. Table 3 presents a sample of the TUTIEMPO data set. Note that the NASA data are available on a mean-monthly basis, whereas the latter data are downloadable on a day-by-day basis. Thus by extension of the present work, one may obtain irradiation estimates for daily irradiation using the TUTIEMPO data. The present article deals with mean-monthly estimates.

This section is concluded by pointing out two things that qualify this study, i.e. (i) NASA data are based on satellite observations that represent inferred values of irradiation. In contrast, TuTiempo provides ground-*measured* data for temperature. Hence, if reliable regressions are available between irradiation and mean temperature, then the latter data may be used to obtain more realistic estimates of irradiation. (ii) TuTiempo provides mean-minimum and maximum temperatures. Those can be used to decompose daily to hourly temperatures.

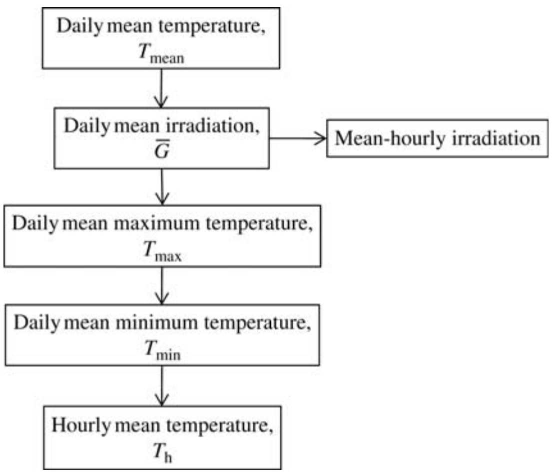

Figure 1. *Flow diagram for obtaining hourly solar irradiation and temperature from mean-daily temperature.*

3 PREVIOUS WORK

As mentioned above, solar radiation can be estimated by means of empirical relations using other available

Table 4. *Locations selected for the present monthly mean database.*

0–20				20–40				40–60			
Location	Latitude	Longitude	Altitude	Location	Latitude	Longitude	Altitude	Location	Latitude	Longitude	Altitude
Accra	5.60	−0.16	68	Makkah	21.43	39.83	310	Barcelona	41.28	2.06	4
Georgetown	6.50	−58.25	29	Aswan	23.96	32.78	200	Rome	41.95	12.50	18
Con Son	8.68	106.58	9	Kufra	24.21	23.30	417	Sofia	42.65	23.38	586
Juan Santamaria	9.98	−84.21	920	Riyadh	24.70	46.71	635	Sapporo	43.06	141.33	26
Barcelona. V	10.11	−64.68	7	Manama	26.26	50.65	2	Varna	43.20	27.91	41
Cartagena	10.45	−75.51	1	Asyut	27.05	31.01	226	San Sebastian	43.35	−1.80	5
Caracas	10.60	−66.98	43	I-n-Salah	27.23	2.46	269	Cannes	43.53	6.95	3
Babanusa	11.33	27.81	453	Cairo	30.13	31.40	64	Toulouse	43.63	1.36	152
Phnom-Penh	11.55	104.85	10	Tripoli	32.66	13.15	80	Florence	43.80	11.20	40
Madras	13.00	80.18	10	Palmyra	34.55	38.30	408	Bologna	44.53	11.30	36
Bangkok	13.66	100.56	4	Aleppo	36.18	37.21	393	Milan	45.43	9.28	107
San Salvador	13.70	−89.11	616	Tunis	36.83	10.23	3	Timisoara	45.76	21.25	86
La Esperanza	14.31	−88.16	1100	Faro	37.01	−7.96	7	Odessa	46.43	30.76	42
Guatemala	14.58	−90.51	1489	Seville	37.41	−5.90	34	Quebec	46.80	−71.38	70
Sanaa	15.51	44.20	2206	Izmir	38.26	27.15	125	Graz	47.00	15.43	340
Abbs	16.08	43.16	2000	Alicante	38.28	−0.55	43	Budapest	47.43	19.26	151
Timbuktu	16.71	−3.00	263	Philadelphia	39.86	−75.23	6	London	51.51	−0.11	5
Acapulco	16.83	−99.93	28	Ankara	39.95	32.88	891	Moscow	55.75	37.63	156
Mexico	19.43	−99.10	2238	Madrid	40.38	−3.78	690	Edinburgh	55.95	−3.35	41
Akola	20.70	77.03	282	Istanbul	40.96	28.81	48	Petersburg	59.96	30.30	4

Note that 20 locations have been selected for each of the three latitude bands: 0–20, 20–40 and 40–60°N.

Table 5. *Sample of data used in the present work.*

Latitude	Cities	January–June						July–December					
		Months	G_{NASA}	$T_{max\text{-}TuTiempo}$	$T_{mean\text{-}NASA}$	$T_{mean\text{-}TuTiempo}$	$T_{min\text{-}TuTiempo}$	Months	G_{NASA}	$T_{max\text{-}TuTiempo}$	$T_{mean\text{-}NASA}$	$T_{mean\text{-}TuTiempo}$	$T_{min\text{-}TuTiempo}$
0–20	Cartagena	January	6.0	30.4	26.7	27.0	24.3	July	5.9	32.3	26.5	28.9	26.4
		February	6.3	30.4	27.4	27.0	24.6	August	5.9	32.4	26.4	29.0	26.7
		March	6.5	30.1	27.7	26.8	24.5	September	5.3	32.5	26.1	29.3	26.9
		April	6.2	31.0	26.8	27.9	25.5	October	5.0	32.4	25.9	29.0	26.7
		May	5.7	31.4	26.4	28.4	26.3	November	5.0	31.9	26.0	28.7	26.4
		June	5.7	31.5	26.6	28.6	26.1	December	5.4	31.8	26.0	28.2	25.5
	Caracas	January	5.4	30.2	24.4	26.7	23.9	July	5.8	33.1	25.0	29.0	26.1
		February	5.8	29.5	24.8	26.2	23.6	August	5.9	33.6	25.2	29.6	26.7
		March	6.2	30.4	25.3	26.7	24.0	September	5.8	34.8	25.4	30.3	27.2
		April	5.8	31.3	25.7	27.8	24.8	October	5.4	33.2	25.3	29.4	26.3
		May	5.5	32.7	25.6	28.7	26.1	November	5.0	32.2	25.1	28.3	25.3
		June	5.5	33.6	25.2	29.1	26.1	December	5.0	30.8	24.7	27.0	24.2
	Babanusa	January	5.7	34.8	23.6	29.1	21.0	July	5.7	33.4	25.1	29.6	24.3
		February	6.3	38.1	25.6	313	21.7	August	5.5	33.3	24.9	29.8	25.4
		March	6.7	37.8	28.5	317	21.9	September	5.9	33.4	26.0	28.7	24.2
		April	7.0	42.1	29.7	36.7	29.8	October	5.8	35.3	27.7	30.7	25.3
		May	6.6	40.1	28.3	35.3	27.4	November	5.8	35.5	27.3	30.4	23.6
		June	6.2	37.6	26.5	32.5	27.3	December	5.5	33.9	24.4	27.5	19.0
	Madras	January	4.9	30.3	26.1	25.1	20.8	July	4.7	37.6	29.5	31.9	27.1
		February	5.9	32.4	27.0	26.6	21.6	August	4.8	35.5	29.4	29.6	25.5
		March	6.6	34.1	27.5	28.5	23.7	September	5.0	35.7	28.5	30.2	25.3
		April	6.7	36.6	27.0	30.8	26.4	October	4.4	34.7	27.0	29.7	25.0
		May	6.1	38.6	26.8	32.1	27.1	November	4.1	30.2	26.1	26.5	23.7
		June	5.2	39.3	26.4	32.3	27.8	December	4.2	28.9	25.5	25.1	22.1
	Makkah	January	4.5	33.2	213	25.8	20.6	July	7.0	44.5	30.9	36.3	29.8
		February	5.3	34.4	217	26.8	21.2	August	6.5	43.6	30.7	35.7	30.2
		March	6.2	35.7	23.5	27.6	21.5	September	6.2	43.5	30.9	34.9	28.8
		April	6.9	40.2	26.3	319	24.6	October	5.6	40.8	28.7	31.7	25.6
		May	7.2	42.6	29.5	33.9	27.8	November	4.6	35.9	25.4	28.4	23.3
		June	7.1	45.4	30.9	37.0	31.0	December	4.2	33.0	22.6	25.4	20.5
20–40	Manama	January	3.6	20.0	18.6	16.0	12.6	July	7.3	38.9	35.1	35.6	32.5
		February	4.4	23.4	19.3	19.2	16.2	August	7.0	39.5	35.2	35.3	32.1
		March	5.1	24.7	215	210	17.8	September	6.5	37.2	33.1	33.3	30.3
		April	6.0	29.9	25.8	25.6	22.0	October	5.3	33.4	29.8	29.7	26.5
		May	7.0	36.9	30.8	319	28.1	November	4.0	28.7	25.4	25.8	23.3
		June	7.7	40.0	33.6	35.3	31.1	December	3.3	22.5	21.1	20.2	17.8
	Asyut	January	3.5	22.0	13.5	13.7	6.2	July	8.0	38.3	30.4	31.7	24.4
		February	4.7	23.6	14.4	15.2	7.1	August	7.5	36.6	30.2	29.9	22.6
		March	6.0	25.0	18.1	17.2	9.2	September	6.6	35.7	28.3	28.5	20.9
		April	7.0	32.1	23.2	24.0	15.5	October	5.2	33.3	24.4	25.6	18.4
		May	7.5	33.4	27.0	26.3	18.3	November	3.8	25.5	19.5	18.1	11.3
		June	8.2	38.2	29.1	30.7	22.3	December	3.1	23.2	15.0	14.9	7.9
	I-n-Salah	January	3.8	21.0	12.0	13.4	6.7	July	7.5	46.1	35.9	38.9	31.6
		February	4.9	24.4	14.9	17.0	9.8	August	7.0	44.9	35.3	37.4	30.2
		March	5.9	29.5	19.4	22.0	15.0	September	5.8	39.3	31.9	31.8	24.0
		April	6.6	33.0	24.1	24.6	15.9	October	4.8	35.9	25.9	28.4	20.6

Continued

Table 5. *Continued*

Latitude	Cities	January–June						July–December					
		Months	G_{NASA}	$T_{max\text{-}TuTiempo}$	$T_{mean\text{-}NASA}$	$T_{mean\text{-}TuTiempo}$	$T_{min\text{-}TuTiempo}$	Months	G_{NASA}	$T_{max\text{-}TuTiempo}$	$T_{mean\text{-}NASA}$	$T_{mean\text{-}TuTiempo}$	$T_{min\text{-}TuTiempo}$
		May	7.1	39.5	29.2	31.9	24.0	November	3.9	28.5	19.0	20.7	12.9
		June	7.3	44.1	33.9	36.8	28.9	December	3.5	26.0	13.5	16.8	8.6
	Istanbul	January	1.7	10.3	4.8	7.4	4.1	July	7.3	30.6	24.1	26.0	21.9
		February	2.5	9.7	5.0	7.0	4.5	August	6.4	29.7	23.9	25.0	20.8
		March	3.7	11.6	7.6	8.5	5.1	September	5.0	25.1	20.8	21.0	16.8
		April	4.8	16.4	12.8	12.0	8.3	October	3.1	21.6	16.0	18.2	14.4
		May	6.3	23.0	17.8	18.4	13.6	November	1.9	15.8	10.4	12.8	8.6
		June	7.2	28.3	22.0	23.4	18.8	December	1.4	13.3	6.1	10.4	6.7
40–60	Barcelona	January	2.1	12.7	9.4	8.6	4.6	July	6.8	28.3	22.9	24.7	21.9
		February	3.1	13.7	9.7	9.4	5.4	August	5.8	30.1	23.2	25.6	22.4
		March	4.3	15.4	11.3	11.8	7.6	September	4.6	25.8	20.8	21.8	18.3
		April	5.3	17.9	13.0	13.9	10.0	October	3.1	22.9	17.7	18.6	14.7
		May	6.0	22.4	16.3	18.3	14.7	November	2.1	19.0	13.2	14.3	10.0
		June	6.7	26.4	20.2	22.2	18.6	December	1.8	13.9	10.6	10.1	6.1
	Sofia	January	1.8	3.8	−2.1	−1.2	−6.2	July	6.2	29.2	21.3	22.3	14.4
		February	2.5	5.6	−0.7	0.7	−3.8	August	5.5	28.8	21.1	21.7	14.7
		March	3.5	11.6	3.6	5.7	0.2	September	4.2	24.0	16.6	17.2	10.9
		April	4.2	19.1	9.3	11.9	4.8	October	2.8	17.9	10.7	12.0	6.3
		May	5.1	24.0	14.7	17.1	9.6	November	1.8	14.3	4.1	7.2	1.0
		June	6.0	27.0	18.8	20.0	12.1	December	1.4	7.8	−1.0	2.6	−19
	Sapporo	January	1.3	1.4	−4.3	−1.4	−5.3	July	4.9	23.0	18.6	19.7	16.8
		February	2.2	0.9	−4.1	−2.2	−6.0	August	4.5	25.3	20.1	21.4	18.3
		March	3.6	4.9	−0.7	1.5	−2.2	September	3.9	22.2	16.6	17.8	13.1
		April	4.8	12.5	4.9	7.8	2.6	October	2.6	16.6	11.1	12.4	7.9
		May	5.5	19.2	10.0	13.9	9.0	November	14	8.3	4.5	5.1	1.4
		June	5.5	21.7	14.8	17.5	14.1	December	1.0	2.2	−1.4	−0.7	−4.1
	Varna	January	1.6	7.4	1.4	2.3	−1.8	July	6.1	30.4	24.2	24.0	17.7
		February	2.4	8.4	2.3	3.8	0.0	August	5.4	28.6	23.8	22.0	15.3
		March	3.3	11.6	6.4	6.4	1.7	September	4.2	25.1	19.8	18.5	12.6
		April	4.3	16.2	11.7	10.4	4.6	October	2.7	19.4	14.5	14.1	9.0
		May	5.5	22.9	17.2	16.3	9.4	November	1.7	15.6	7.7	9.9	5.6
		June	6.0	27.7	21.7	21.1	13.9	December	1.3	9.5	2.5	4.9	10
	San Sebastian	January	1.6	12.3	6.1	9.0	4.6	July	6.3	25.1	21.3	21.3	17.3
		February	2.3	12.5	6.7	9.4	5.0	August	5.5	25.4	21.4	21.6	18.1
		March	3.7	14.9	9.2	11.6	7.0	September	4.3	22.8	18.7	19.2	15.7
		April	4.7	16.7	11.2	12.5	8.6	October	2.8	21.4	15.0	16.6	12.5
		May	5.7	19.6	15.5	15.8	12.5	November	1.7	17.9	9.9	14.1	9.7
		June	6.2	24.1	19.2	20.0	15.9	December	1.3	12.7	7.3	9.6	6.0

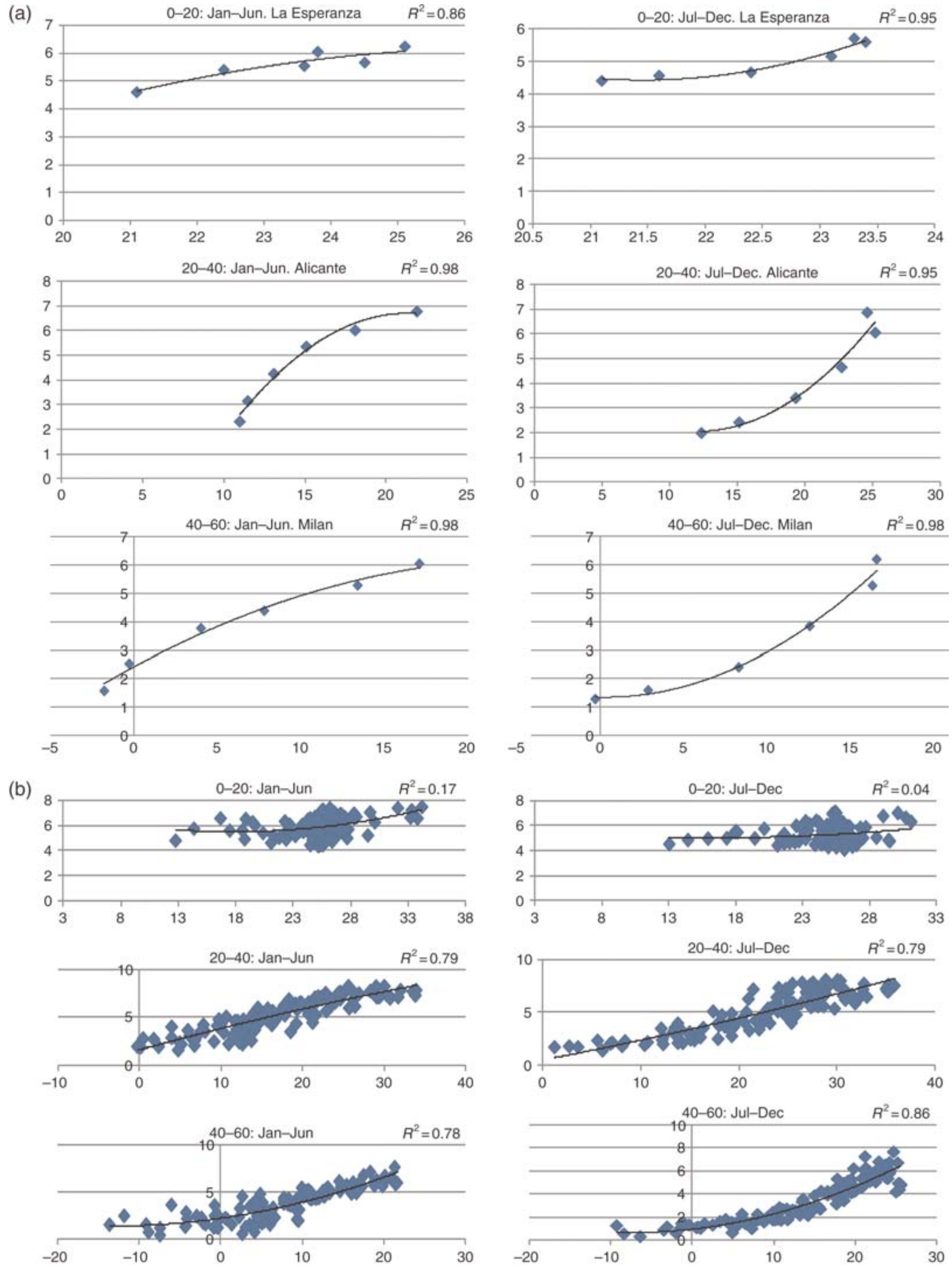

Figure 2. *(a) Regression between mean-daily irradiation ($\overline{G}$) and temperature (T_{mean}) for three locations.* x-axis: *T_{mean} and y-axis: $\overline{G}$. (b) Regression between mean-daily irradiation ($\overline{G}$) and temperature (T_{mean}): all locations. x-axis: T_{mean} and y-axis: $\overline{G}$.*

meteorological observations such as (a) mean-daily sunshine duration, (b) cloud-cover, (c) ambient temperature along with precipitation and/or humidity or (d) ambient temperature as the sole regressor. An exhaustive review of the above methods is available in standard references [4–6]. In this article, effort has been concentrated on models that exclusively deal with ambient temperature as the sole predictor or regressor and as such models dealing with other meteorological parameters are not dealt here. The theme of the present work stems from the logic that temperature records have existed for a very long time and also the measurement network is indeed very wide. Hence an irradiation model of the type that is presently proposed would be of benefit, particularly for those in the developing countries where there is a dearth of measured irradiation data.

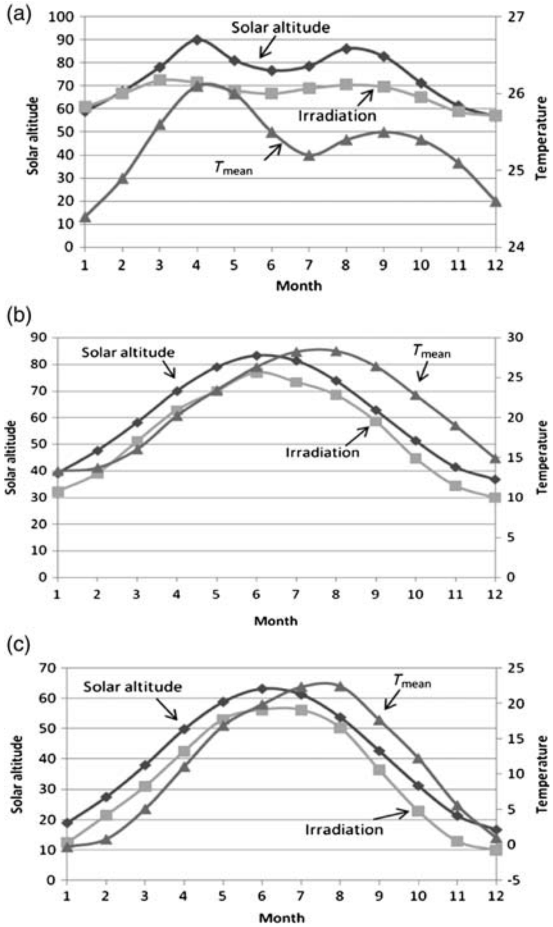

Figure 3. *Solar altitudes at noon, irradiation (×10) and T_{mean} at (a) 10° latitude, (b) 30° latitude and (c) 50° latitude.*

Even for the sparse irradiation network, there is the challenge of careful maintenance of solarimeters that is required on a day-to-day basis, particularly the due care that is associated with diffuse radiation measurement. In this respect, a discussion on the lack of care of shade-ring adjustment and the corresponding errors has been enumerated by Muneer [6].

As pointed out above, solar radiation affects the earth's weather processes. After cooling of the land mass during the night, sensible heating resulting from irradiation absorption effects is responsible for ambient temperature variations, so it is possible to obtain a relationship between temperature and solar radiation. The landmark work in this respect was carried out by Campbell [7]. Using this argument, Bristow and Campbell [8] suggested a relationship for global solar radiation as a function of irradiation and the difference between maximum and minimum temperature.

Hargreaves and Samani [9] suggested that solar radiation can be estimated from the above-mentioned difference between the maximum and minimum air temperatures, and introduced an empirical coefficient K_r. Hargreaves [10] recommended the value of K_r to be 0.16 for interior regions and 0.19 for coastal regions. Annandale *et al.* [11] introduced a correction factor

Table 6. *Comparison between the findings of Bandyopadhyay et al. [24] using Equation (1) and the present developed model.*

Station	ME	RMSE (%)
Ahmedabad	0.89	6.4
Amritsar	0.92	7.9
Bhopal	0.73	12.7
Hyderabad	0.78	8.6
Jaipur	0.31	16.8
Kodaikanal	0.77	10.1
Nagpur	0.93	4.9
Okha	0.39	13.2
Pune	0.89	6.0
Shillong	0.71	9.9
Present work		
Sanaa	−8.19	19.2
Kufra	0.74	11.5
Budapest	0.92	13.9

for the empirical coefficient to account for effects of reduced atmospheric thickness on solar radiation. Allen [12] obtained K_r as a function of the location altitude to take account of the volumetric heat capacity of the atmosphere (Equation 1).

Allen [13] suggested the use of a self-calibrating model to estimate mean monthly global solar radiation following the work of Hargreaves and Samani [9]. Samani [14] developed an empirical relationship between K_r and the difference between air temperature extremes. Meza and Varas [15] evaluated the behaviour of the models of Allen [13] and Bristow and Campbell [8] and inter-compared their results.

Using data from 40 stations covering contrasting climates, Thornton and Running [1] present a reformulation of the Bristow and Campbell model for daily solar radiation, based on daily observations of temperature, humidity and precipitation.

Liu and Scott [16] evaluated the accuracy and applicability of several models for estimating daily value of solar radiation across Australia for different situations, i.e. using the work of McCaskill [17,18] when only rainfall data were available, the work of Bristow and Campbell [8], Richardson [19] and Hargreaves and Riley [20] when only temperature data were available, and the work of De Jong and Stewart [21] and Hunt *et al.* [22] when data for rainfall and temperature were available.

Zhoy *et al.* [23] validated and compared the above models to predict monthly average daily global radiation on a horizontal surface based on data from 69 meteorological stations in China. Their work was then extended to select the model with the highest accuracy that was then deployed to obtain a geographical distribution of solar radiation across China.

In their landmark work, Bandyopadhyay *et al.* [24] estimated solar radiation by using nearly all of the above models that deal with temperature as the sole predictor and reported on the relative accuracy of those models. The work of Bandyopadhyay *et al.* [24] was based on data from 29 stations that were distributed throughout India. The methods

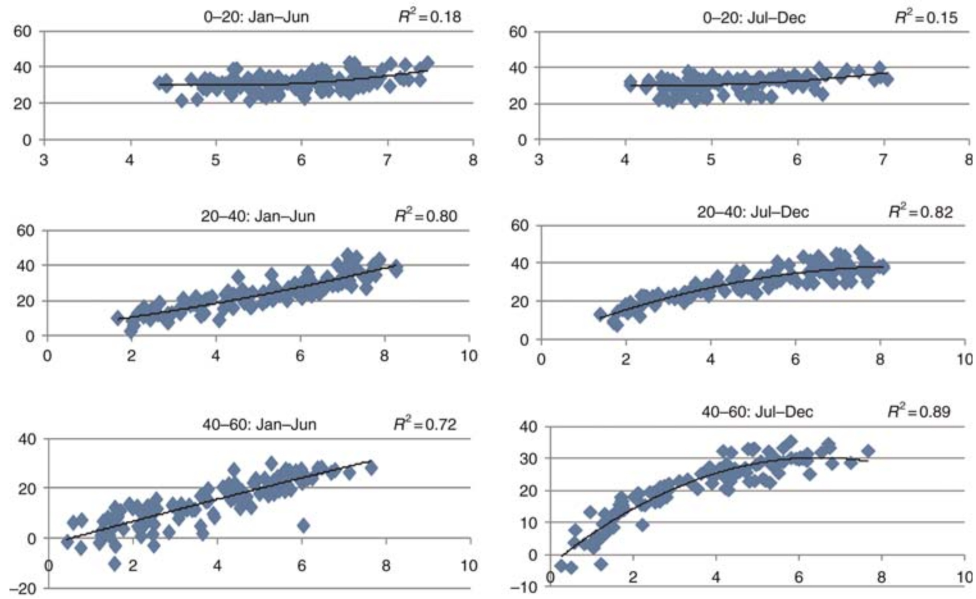

Figure 4. *Regression between mean-daily irradiation ($\overline{G}$) and maximum temperature (T_{max}): all locations. x-axis: $\overline{G}$ and y-axis: T_{max}.*

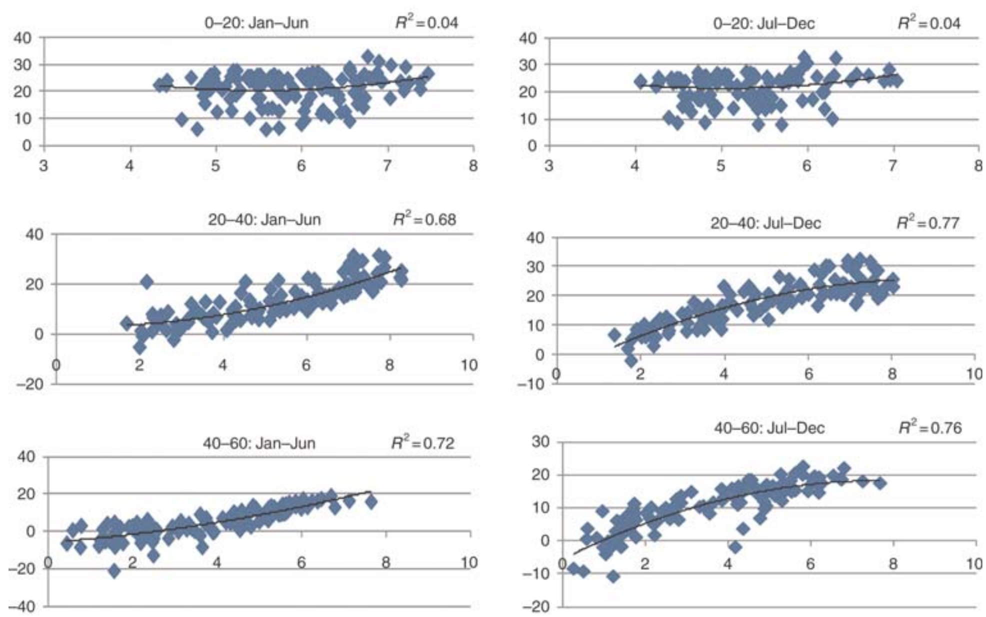

Figure 5. *Regression between mean-daily irradiation ($\overline{G}$) and minimum temperature (T_{min}): all locations. x-axis: $\overline{G}$ and y-axis: T_{min}.*

compared were Hargreaves [10], Annandale *et al.* [11], Allen [12,13], Samani [14] and Bristow and Campbell [8]. The estimated solar radiation values were then compared with measured solar radiation (or solar radiation estimated from measured sunshine hours with locally calibrated Angstrom coefficients), to check the suitability of these methods under Indian conditions. The conclusion drawn by Bandyopadhyay *et al.* [24] was that the original Hargreaves [10] method performed overall best for Indian locations. The methods due to Allen [12], Samani [14] and Bristow and Campbell [8] were found to be inferior with the latter being the poorest of the lot. The Hargreaves [10] method may be summarized thus,

$$\bar{G} = K_r (T_{max} - T_{min})^{0.5} \bar{E} \qquad (1)$$

where $\overline{G}$ is the monthly-mean daily extraterrestrial irradiation (kWh/m^2).

Table 7. *Regression between mean-daily irradiation ($\overline{G}$) and temperature (T_{mean}): all locations.*

0–20				20–40				40–60			
Location	Latitude	$\overline{G} - T_{\mathrm{mean}}$		Location	Latitude	$\overline{G} - T_{\mathrm{mean}}$		Location	Latitude	$\overline{G} - T_{\mathrm{mean}}$	
		R^2				R^2				R^2	
		January–June	July–December			January–June	July–December			January–June	July–December
Accra	5.60	0.80	0.91	Makkah	21.43	0.97	0.94	Barcelona	41.28	0.96	0.96
Georgetown	6.50	0.07	0.56	Aswan	23.96	0.96	0.98	Rome	41.95	0.97	0.97
Con Son	8.68	0.71	0.66	Kufra	24.21	0.96	0.98	Sofia	42.65	0.96	0.99
Juan Santamaria	9.98	0.51	0.20	Riyadh	24.70	0.99	0.99	Sapporo	43.06	0.97	0.97
Barcelona. V	10.11	0.75	0.69	Manama	26.26	0.98	0.99	Varna	43.20	0.99	0.99
Cartagena	10.45	0.86	0.93	Asyut	27.05	0.97	1.00	San Sebastian	43.35	0.99	0.98
Caracas	10.60	0.25	0.35	I-n-Salah	27.23	1.00	0.99	Cannes	43.53	0.98	0.97
Babanusa	11.33	0.95	0.81	Cairo	30.13	0.98	0.99	Toulouse	43.63	0.99	0.99
Phnom-Penh	11.55	0.46	0.87	Tripoli	32.66	0.98	0.92	Florence	43.80	0.99	0.98
Madras	13.00	0.95	0.77	Palmyra	34.55	0.99	0.99	Bologna	44.53	0.99	0.98
Bangkok	13.66	0.49	0.94	Aleppo	36.18	0.99	0.99	Milan	45.43	0.98	0.98
San Salvador	13.70	0.60	0.98	Tunis	36.83	0.97	0.96	Timisoara	45.76	0.99	0.99
La Esperanza	14.31	0.86	0.95	Faro	37.01	0.99	0.99	Odessa	46.43	0.99	0.99
Guatemala	14.58	0.46	0.77	Seville	37.41	0.99	0.99	Quebec	46.80	0.98	1.00
Sanaa	15.51	0.99	0.91	Izmir	38.26	0.98	0.99	Graz	47.00	0.99	0.99
Abbs	16.08	0.99	0.85	Alicante	38.28	0.98	0.95	Budapest	47.43	0.99	0.99
Timbuktu	16.71	0.99	0.77	Philadelphia	39.86	0.99	1.00	London	51.51	0.99	0.99
Acapulco	16.83	0.60	0.83	Ankara	39.95	0.97	0.99	Moscow	55.75	0.96	1.00
Mexico	19.43	0.73	0.86	Madrid	40.38	0.99	0.99	Edinburgh	55.95	0.99	0.99
Akola	20.70	0.79	0.00	Istanbul	40.96	0.98	0.99	Petersburg	59.96	0.98	1.00

Table 8. *Regression between mean-daily irradiation ($\overline{G}$) and maximum temperature (T_{max}): all locations.*

0–20				20–40				40–60			
Location	Latitude	$T_{\mathrm{max}} - \overline{G}$		Location	Latitude	$T_{\mathrm{max}} - \overline{G}$		Location	Latitude	$T_{\mathrm{max}} - \overline{G}$	
		R^2				R^2				R^2	
		January–June	July–December			January–June	July–December			January–June	July–December
Accra	5.60	0.95	0.86	Makkah	21.43	0.93	1.00	Barcelona	41.28	0.99	0.96
Georgetown	6.50	0.09	0.38	Aswan	23.96	0.98	0.98	Rome	41.95	0.98	0.96
Con Son	8.68	0.47	0.32	Kufra	24.21	0.94	0.98	Sofia	42.65	0.98	0.97
Juan Santamaria	9.98	0.23	0.44	Riyadh	24.70	0.99	0.99	Sapporo	43.06	1.00	0.98
Barcelona. V	10.11	0.28	0.17	Manama	26.26	0.99	0.99	Varna	43.20	1.00	0.98
Cartagena	10.45	0.78	0.13	Asyut	27.05	0.98	0.99	San Sebastian	43.35	0.98	0.93
Caracas	10.60	0.17	0.78	I-n-Salah	27.23	0.98	0.99	Cannes	43.53	0.98	0.99
Babanusa	11.33	0.83	0.36	Cairo	30.13	1.00	0.97	Toulouse	43.63	0.98	0.98
Phnom-Penh	11.55	0.47	0.65	Tripoli	32.66	0.99	0.99	Florence	43.80	0.97	0.98
Madras	13.00	0.16	0.77	Palmyra	34.55	1.00	0.98	Bologna	44.53	0.99	0.98
Bangkok	13.66	0.70	0.16	Aleppo	36.18	0.99	0.98	Milan	45.43	0.99	0.99
San Salvador	13.70	0.91	0.68	Tunis	36.83	0.99	0.99	Timisoara	45.76	0.96	0.98
La Esperanza	14.31	0.51	0.57	Faro	37.01	0.97	0.97	Odessa	46.43	0.98	0.98
Guatemala	14.58	0.44	0.73	Seville	37.41	0.99	0.95	Quebec	46.80	0.99	0.92
Sanaa	15.51	0.92	0.59	Izmir	38.26	0.99	0.99	Graz	47.00	0.99	0.98
Abbs	16.08	0.91	0.86	Alicante	38.28	0.99	0.96	Budapest	47.43	0.96	0.99
Timbuktu	16.71	0.96	0.81	Philadelphia	39.86	0.99	0.97	London	51.51	0.98	0.97
Acapulco	16.83	0.46	0.80	Ankara	39.95	0.98	0.96	Moscow	55.75	1.00	0.97
Mexico	19.43	0.73	0.78	Madrid	40.38	0.97	0.97	Edinburgh	55.95	0.97	0.96
Akola	20.70	0.77	0.52	Istanbul	40.96	1.00	0.99	Petersburg	59.96	1.00	0.98

Table 9. *Regression between mean-daily irradiation ($\overline{G}$) and minimum temperature (T_{min}): all locations.*

0–20				20–40				40–60			
Location	Latitude	$T_{min} - \overline{G}$ R^2		Location	Latitude	$T_{min} - \overline{G}$ R^2		Location	Latitude	$T_{min} - \overline{G}$ R^2	
		January–June	July–December			January–June	July–December			January–June	July–December
Accra	5.60	0.72	0.85	Makkah	21.43	0.85	0.97	Barcelona	41.28	0.99	0.98
Georgetown	6.50	0.63	0.21	Aswan	23.96	0.99	0.99	Rome	41.95	0.99	0.98
Con Son	8.68	0.64	0.07	Kufra	24.21	0.95	1.00	Sofia	42.65	0.99	1.00
Juan Santamaria	9.98	0.69	0.90	Riyadh	24.7	0.99	0.98	Sapporo	43.06	0.96	0.98
Barcelona. V	10.11	0.17	0.46	Manama	26.26	0.99	0.98	Varna	43.2	0.99	0.97
Cartagena	10.45	0.69	0.15	Asyut	27.05	0.99	0.99	San Sebastian	43.35	0.99	0.98
Caracas	10.60	0.18	0.83	I-n-Salah	27.23	0.94	0.99	Cannes	43.53	0.98	0.97
Babanusa	11.33	0.39	0.18	Cairo	30.13	0.99	0.98	Toulouse	43.63	1.00	0.94
Phnom-Penh	11.55	0.31	0.86	Tripoli	32.66	0.99	0.99	Florence	43.8	0.95	0.98
Madras	13.00	0.11	0.55	Palmyra	34.55	1.00	0.98	Bologna	44.53	0.98	0.94
Bangkok	13.66	0.20	0.01	Aleppo	36.18	0.99	0.98	Milan	45.43	0.98	0.97
San Salvador	13.70	0.22	0.75	Tunis	36.83	0.99	1.00	Timisoara	45.76	0.99	0.98
La Esperanza	14.31	0.28	0.57	Faro	37.01	0.95	0.98	Odessa	46.43	0.97	0.96
Guatemala	14.58	0.09	0.90	Seville	37.41	0.96	0.98	Quebec	46.8	0.99	0.94
Sanaa	15.51	0.96	0.55	Izmir	38.26	0.98	0.99	Graz	47	1.00	0.98
Abbs	16.08	0.90	0.81	Alicante	38.28	0.99	0.99	Budapest	47.43	0.98	0.98
Timbuktu	16.71	0.88	0.97	Philadelphia	39.86	1.00	0.94	London	51.51	0.98	0.94
Acapulco	16.83	0.26	0.66	Ankara	39.95	0.98	0.96	Moscow	55.75	0.97	0.92
Mexico	19.43	0.34	0.66	Madrid	40.38	0.97	0.98	Edinburgh	55.95	0.98	0.97
Akola	20.70	0.24	0.31	Istanbul	40.96	1.00	0.98	Petersburg	59.96	1.00	0.93

Table 10. *Models for mean-daily irradiation ($\overline{G}$) based on mean temperature (T_{mean}), mean-maximum temperature (T_{max}) based on daily irradiation ($\overline{G}$) and mean-minimum temperature (T_{min}) based on daily irradiation ($\overline{G}$): all locations.*

Latitude range	January–June		July–December	
	Model	R^2	Model	R^2
$\overline{G}$ based on T_{mean}				
0–20	$\bar{G} = 7.52 - 0.23 \times T_{mean} + 0.01 \times T_{mean}^2$	0.17	$\bar{G} = 5.837 - 0.102 \times T_{mean} + 0.003 \times T_{mean}^2$	0.04
20–40	$\bar{G} = 1.636 + 0.232 \times T_{mean} - 0.001 \times T_{mean}^2$	0.79	$\bar{G} = 0.511 + 0.175 \times T_{mean} + 0.001 \times T_{mean}^2$	0.79
40–60	$\bar{G} = 2.211 + 0.123 \times T_{mean} + 0.005 \times T_{mean}^2$	0.78	$\bar{G} = 0.955 + 0.078 \times T_{mean} + 0.005 \times T_{mean}^2$	0.86
T_{max} based on $\overline{G}$				
0–20	$T_{max} = 67.61 - 14.81 \times \bar{G} + 1.45 \times \bar{G}^2$	0.18	$T_{max} = 50.70 - 9.39 \times \bar{G} + 1.06 \times \bar{G}^2$	0.15
20–40	$T_{max} = 4.19 + 2.83 \times \bar{G} + 0.18 \times \bar{G}^2$	0.8	$T_{max} = 0.15 + 8.80 \times \bar{G} - 0.50 \times \bar{G}^2$	0.82
40–60	$T_{max} = -2.47 + 4.66 \times \bar{G} - 0.04 \times \bar{G}^2$	0.72	$T_{max} = -3.06 + 10.30 \times \bar{G} - 0.80 \times \bar{G}^2$	0.89
T_{min} based on $\overline{G}$				
0–20	$T_{min} = 59.33 - 14.17 \times \bar{G} + 1.29 \times \bar{G}^2$	0.04	$T_{min} = 2.89 - 0.36 \times \bar{G} + 0.39 \times \bar{G}^2$	0.04
20–40	$T_{min} = 52.48 - 12.45 \times \bar{G} + 1.24 \times \bar{G}^2$	0.68	$T_{min} = -6.52 + 7.17 \times \bar{G} - 0.40 \times \bar{G}^2$	0.77
40–60	$T_{min} = -5.89 + 1.66 \times \bar{G} + 0.25 \times \bar{G}^2$	0.72	$T_{min} = -5.45 + 6.19 \times \bar{G} - 0.40 \times \bar{G}^2$	0.76

4 PRESENTLY PROPOSED MODELS

The present work is developed around the philosophy that for a great many locations around the world, the only parameter that may be available is the mean ambient temperature. Furthermore, the model is simple in its constitution. It has been constructed with the ease of use in mind. Presently, three types of models are proposed that, respectively, deal with (i) mean-daily irradiation, (ii) mean-hourly irradiation and (iii) hourly temperature. These are presented in the subsequent sections. Figure 1 shows the information flow diagram for the present computational scheme.

4.1 Models for mean-daily irradiation

Table 4 presents a list of all locations that have been selected for the present monthly-mean database. Note that 20 locations have been selected for each of the three latitude bands: 0–20,

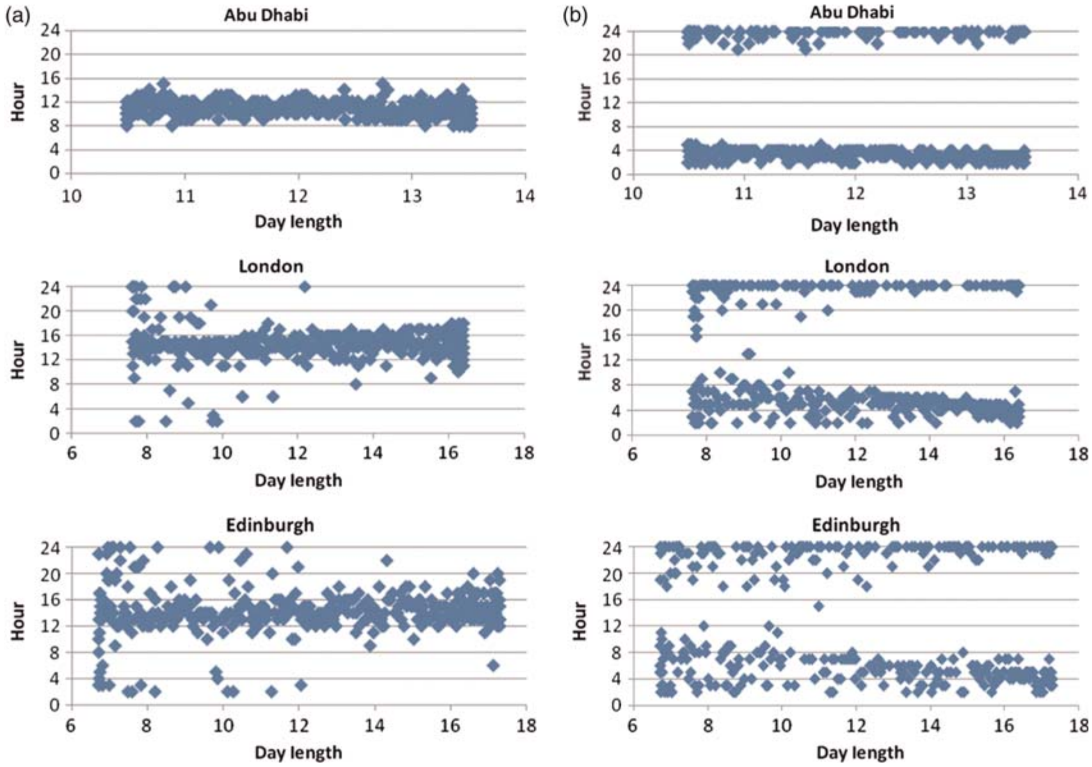

Figure 6. *Time of occurrence of the (a) maximum and (b) minimum temperature.*

20–40 and 40–60°N. The temporal split was created in two broad categories, i.e. the heating period represented by the January–June months and the cooling by the July–December period. For the southern hemisphere, the split would obviously be reversed. The present study, being the first of its kind, is being restricted to the northern hemisphere and an extension may easily be undertaken for the southern part of the globe as pointed out above.

Data were extracted from two sources, i.e. the NASA and the TuTiempo websites. The former website provides information on $\overline{G}$ and T_{mean}. However, to obtain hourly temperatures, one needs mean-daily T_{min} and T_{max}. Hence, the latter data were obtained from the TuTiempo website. A sample of the pooled data is shown in Table 5. The next step was to obtain regressions between $\overline{G}$ and T_{mean}, the logic being that T_{mean} is available much more widely in terms of spatial and temporal coverage as pointed out in Section 1.

Figure 2a and b, respectively, shows regressions between $\overline{G}$ and T_{mean} for individual and grouped locations. Two points are worth mentioning. First, for any given location, there is a strong correlation between the two parameters under discussion and, secondly, the high values of R^2 are restricted to latitudes above 20°. The much more weaker correlations for the near-equatorial band have also been reported by Swartman and Ogunlade [25] and Bandyopadhyay *et al.* [24]. The former study has, respectively, attempted regressions between $\overline{G}$ and precipitable water and between $\overline{G}$ and daily temperature range. However, the important point to note is that the T_{mean} itself or indeed the daily temperature range is dictated by the much more uniform movement of the sun within the tropics. This point is demonstrated via Figure 3 that shows the narrow range of noon solar altitude for the 0–20° latitude band. Note that for the other two latitude bands 20–40 and the 40–60°, there is a close concordance between T_{mean} and $\overline{G}$ with noon altitude.

The present sets of models were also compared in terms of their accuracy with those reported by Bandyopadhyay *et al.* [24]. The latter team has used the following statistical parameters to evaluate the model's accuracy. Equations for modelling efficiency (ME) and root-mean square error (RMSE), used by the latter work of reference, are provided in the following equations.

$$\mathrm{ME} = \frac{\sum_{i=1}^{n}(x_{o,i}-\overline{x_o})^2 - \sum_{i=1}^{n}(x_{p,i}-x_{o,i})^2}{\sum_{i=1}^{n}(x_{o,i}-\overline{x_o})^2} \quad (2)$$

$$\mathrm{RMSE}\ (\%) = \frac{\left(\sum_{i=1}^{n}(x_{p,i}-x_{o,i})^2/n\right)^{0.5}}{\overline{x_o}} \times 100 \quad (3)$$

where $x_{o,i}$ is the measured variable, $\overline{x_o}$ the average of the measured variable and $x_{p,i}$ the computed variable.

Table 6 compares the findings of Bandyopadhyay *et al.* [24] using Equation (1) and the presently developed model.

Refer to Figure 1 that shows the presently proposed computational chain for obtaining hourly temperatures. The next step is to obtain regression models between T_{max} and $\overline{G}$, and

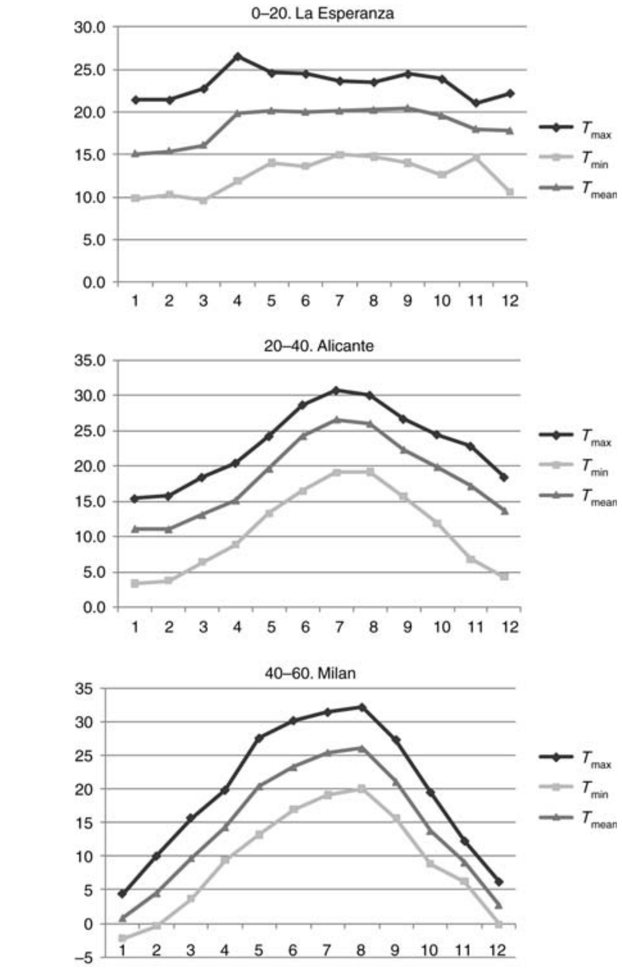

Figure 7. *Inter-relationship between daily maximum, minimum and mean temperature for three locations.*

between T_{min} and $\overline{G}$. Figures 4 and 5, respectively, present those findings. Once again the strong correlation between the variables under discussion is apparent. Furthermore, we note that, as found above, a much weaker correlation exists for the near-equatorial band. Tables 7–9 provide the R^2 values for the regressions under discussion, for all locations. The above discussion is thus further reinforced. It is therefore recommended that the presently proposed relationships be used, with confidence, for locations above 20°N latitude.

Table 10 provides the proposed models that relate $\overline{G}$ to T_{mean}, T_{max} to $\overline{G}$ and T_{min} to $\overline{G}$. Note that there is a weaker correlation between T_{min} and $\overline{G}$. This may be explained as follows. Whereas during the daytime, the sun's irradiation is the strongest contributor to the rise of temperature, after sunset, during nocturnal hours, a number of factors determine the rate of heat loss from the landmass, i.e. direction and speed of wind, and duration and amount of precipitation (rain or snow). Thus a weaker correlation exists between T_{min} and $\overline{G}$. This point is demonstrated in a greater detail in Figure 6a and b. The time of occurrence for T_{max} is much more well defined

Table 11. *Regression between daily-mean minimum temperature: computed and measured values for three locations.*

Cities	Latitude	$T_{computed} - T_{observed}$			
		January–June		July–December	
		Slope	R^2	Slope	R^2
Cartagena	0–20	1.16	0.97	0.99	0.95
I-n-Salah	20–40	1.06	1.00	1.03	1.00
Sofia	40–60	1.06	1.00	1.07	1.00

than T_{min}. The time of occurrence for T_{max} and T_{min} is important information as it enables one to obtain hourly temperatures for the 24 h period. American Society of Heating, Refrigerating and Air-Conditioning Engineers (ASHRAE) [26] has provided the latter procedure and that will be the subject of discussion in Section 4.3.

To provide a better procedure to obtain T_{min}, an attempt was made to relate the latter parameter to T_{mean} and T_{max}. Figure 7 shows the plots for three international locations. The point to note here is that T_{mean} seems to be a close average of T_{min} and T_{max}. On the latter basis, T_{min} may thus be obtained as follows:

$$T_{min} = 2T_{mean} - T_{max} \tag{4}$$

Using Equation (4), T_{min} was computed for three of the present locations and then compared with its measured value. Table 11 shows that using this procedure, T_{min} may be obtained with satisfactory accuracy.

Table 12 shows the correspondence between the T_{mean} values from the two sources—NASA and TuTiempo. Once again we note that there is a much weaker correspondence for locations near the equatorial belt. The primary reason for this may be attributed to the poor quality of measured temperature records for developing countries. A number of studies have alluded to this point. The correspondence at latitudes north of 20° seems to be quite strong though and hence the T_{mean} data may be used inter-changeably.

4.2 Models for mean-hourly irradiation

To provide a model to decompose averaged daily to averaged hourly values, Liu and Jordan [27] built on an earlier work by Whillier [28] to develop a set of regression curves, which represent the ratio of hourly to daily global solar irradiation at a series of time intervals from solar noon. This approach was validated by Collares-Pereira and Rabl [29] who obtained the following equation using a least-square fit as follows:

$$r_G = \frac{\pi}{24}(a + b\cos\omega)\frac{\cos\omega - \cos\omega_s}{\sin\omega_s - \omega_s\cos\omega_s} \tag{5}$$

where r_G is the ratio of hourly to daily global radiation, a and

Table 12. *Regression between monthly-mean temperature (T_{mean}) data from the two sources—NASA and TUTIEMPO.*

0–20				20–40				40–60			
Location	Latitude	$T_{mean\text{-}TuTiempo} - T_{mean\text{-}NASA}$		Location	Latitude	$T_{mean\text{-}TuTiempo} - T_{mean\text{-}NASA}$		Location	Latitude	$T_{mean\text{-}TuTiempo} - T_{mean\text{-}NASA}$	
		Slope	R^2			Slope	R^2			Slope	R^2
Accra	5.60	0.61	0.90	Makkah	21.43	1.09	0.94	Barcelona	41.28	1.17	0.99
Georgetown	6.50	0.39	0.47	Aswan	23.96	1.06	0.98	Rome	41.95	1.20	0.95
Con Son	8.68	0.51	0.79	Kufra	24.21	0.97	0.97	Sofia	42.65	1.05	0.99
Juan Santamaria	9.98	0.90	0.36	Riyadh	24.7	1.07	0.99	Sapporo	43.06	0.98	0.99
Barcelona. V	10.11	0.48	0.33	Manama	26.26	1.12	0.99	Varna	43.20	1.13	0.99
Cartagena	10.45	−0.52	0.65	Asyut	27.05	0.94	0.98	San Sebastian	43.35	1.21	0.98
Caracas	10.60	0.15	0.27	I-n-Salah	27.23	0.99	0.99	Cannes	43.53	1.08	0.98
Babanusa	11.33	0.56	0.65	Cairo	30.13	0.93	0.97	Toulouse	43.63	1.07	0.99
Phnom-Penh	11.55	0.35	0.35	Tripoli	32.66	0.80	0.96	Florence	43.80	0.92	0.98
Madras	13.00	0.63	0.90	Palmyra	34.55	1.01	0.98	Bologna	44.53	0.85	0.98
Bangkok	13.66	0.59	0.49	Aleppo	36.18	0.95	0.98	Milan	45.43	1.12	0.99
San Salvador	13.70	0.65	0.51	Tunis	36.83	0.89	0.98	Timisoara	45.76	1.01	0.98
La Esperanza	14.31	0.34	0.30	Faro	37.01	1.00	0.97	Odessa	46.43	1.06	0.99
Guatemala	14.58	0.43	0.31	Seville	37.41	0.99	0.98	Quebec	46.80	1.06	0.97
Sanaa	15.51	0.78	0.74	Izmir	38.26	1.03	0.99	Graz	47.00	1.03	0.98
Abbs	16.08	0.73	0.69	Alicante	38.28	0.91	0.97	Budapest	47.43	0.98	0.98
Timbuktu	16.71	0.76	0.89	Philadelphia	39.86	0.98	0.98	London	51.51	0.91	0.95
Acapulco	16.83	0.23	0.31	Ankara	39.95	0.96	0.97	Moscow	55.75	1.14	0.98
Mexico	19.43	1.09	0.91	Madrid	40.38	1.01	0.99	Edinburgh	55.95	0.97	0.95
Akola	20.70	0.88	0.91	Istanbul	40.96	0.92	0.97	Petersburg	59.96	1.09	0.98

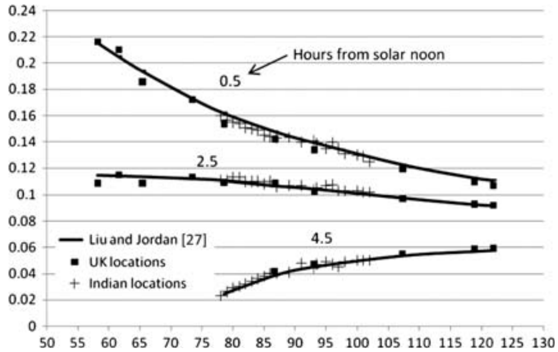

Figure 8. *Ratio of hourly to daily global irradiation for different hours of the day versus sunset hour angle.*

Table 13. *ASHRAE model for diurnal temperature swing.*

Hour	Z	Hour	Z
1	0.12	13	0.95
2	0.08	14	1.00
3	0.05	15	1.00
4	0.02	16	0.94
5	0.00	17	0.86
6	0.02	18	0.76
7	0.09	19	0.61
8	0.26	20	0.50
9	0.45	21	0.41
10	0.62	22	0.32
11	0.77	23	0.25
12	0.87	24	0.18

Table 14. *Performance of ASHRAE model for three international locations.*

Location	Year	Slope	R^2	MBE (°C)	RMSE (°C)
Abu Dhabi	1997	0.99	0.77	−0.1	3.7
London	1990	0.97	0.93	−0.4	1.6
Edinburgh	1990	0.97	0.86	−0.3	1.7

b the site-specific coefficients, ω the hour angle (°) and ω_s the sunset hour angle (°).

In Equation (5), $a = 0.409 + 0.5016 \sin(\omega_s - 1.047)$, $b = 0.6609 - 0.4767 \sin(\omega_s - 1.047)$.

All of the above studies were undertaken using data from US locations. However, the above model's validity was also checked for Indian locations by Hawas and Muneer [30] who compared measurements from 13 Indian locations and found a general agreement for the r_G model. In an extended study, Tham *et al.* [31] used long-term hourly irradiation data from 16 locations in the UK to evaluate the above r_G model. The findings of the above two studies, for India and the UK, are summarized in Figure 8 which shows a remarkable concordance between the r_G model and data from the latter two countries. Tham *et al.* have also reported on the statistical evaluation of the r_G model. The errors in computing hourly from the mean-daily irradiation, for mainland UK locations, were found to be normally distributed around zero, with 39% points lying in the ±10% range, and 67% of the data in the ±20% range.

4.3 Models for hourly temperature

Accurate hourly data are required in very many applications. To meet this need, a simple model to estimate hourly temperature from daily records has been provided by the ASHRAE [32]. A computer program to decompose daily to hourly temperature has been provided by Muneer *et al.* [33]. That code is also available in Muneer's book [6]. The daily maximum temperature that is achieved at a given location is dependent on the prevailing solar radiation, cloud-cover and wind profile. The earliest available models suggest a sinusoidal profile between the daily maximum and minimum temperatures. However, more recent work of Hedrick [34], Thevenard [35] and ASHRAE [26] has further updated the latter model. Table 13 gives the hourly temperature profile, expressed in terms of a presently defined Z-parameter (ratio of hourly temperature elevation to daily range $\{=(T_h - T_{min})/(T_{max} - T_{min})\}$, dimensionless). ASHRAE [26] has suggested that this profile is a representative of both dry-bulb and wet-bulb temperature variation on typical design days. The tabulated information provided by ASHRAE [26] has been cross-checked using averaged hourly data from 58 Turkish locations [36] and hourly data from three international locations, i.e. Edinburgh, London and Abu Dhabi. Table 14 includes that information.

Data from the above three international locations were then used to evaluate the ASHRAE model. Figure 9 and Table 14 present the evaluation that used four statistical indicators. These indicators are the slope of the best-fit regression line between the computed and measured values, coefficient of determination value (R^2) for the above best-fit line, mean bias error (MBE) and RMSE.

The slope of the best-fit line shows that the model performs well for all locations in this study. The R^2 indicator for Abu Dhabi showed that the model slightly under-performs in terms of data scatter. For the remaining stations, the R^2 values lie in the range 0.86–0.93, showing that the model performs well. The highest value of MBE is −0.4°C for Edinburgh and the lowest is −0.1°C at Abu Dhabi. This shows a good agreement with the slope of the best-fit line where Abu Dhabi has the best value near to the desire value of 1. The RMSE value for Abu Dhabi is the highest with the value of 3.7°C and the lowest value of 1.6°C was found for London.

Furthermore, a comparison between the ASHRAE temperature model and the mean-hourly temperature record for locations within the UK and Turkey was carried out. It is evident that the UK temperature trend very closely follows the

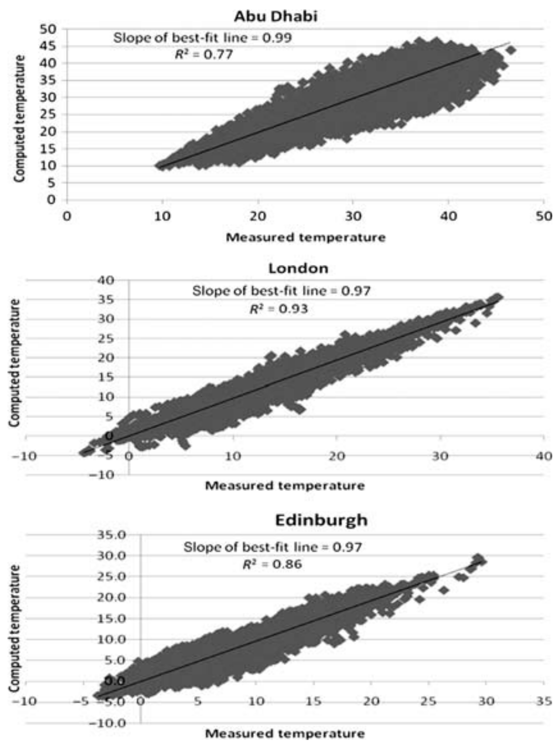

Figure 9. *Presently obtained, yearly averaged Z-parameter for three international locations.*

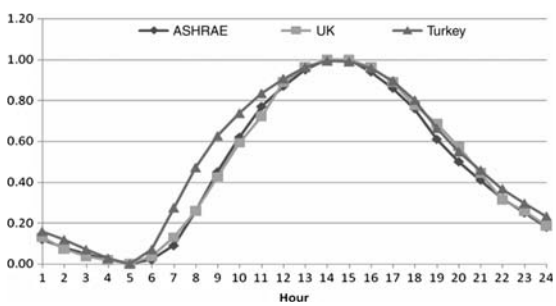

Figure 10. *Comparison of mean-hourly temperature trend.*

ASHRAE model. A slight upward shift of temperatures was observed for Turkey for the ante meridiem hours. Figure 10 shows that comparison.

5 CONCLUSIONS

World-wide there are many more temperature measuring meteorological stations than those that measure solar radiation. Presently, a case has been made for the development of temperature-based mathematical models to obtain mean-daily irradiation. In contrast to the classical models that use daily temperature range, use was made of mean-daily temperature as the basic regressor. The accuracy of predicting mean-daily irradiation was evaluated using two statistical indicators—ME and RMSE. The latter have been defined by Equations (2 and 3). It was found that the ME lay between 0.7 and −8.2% and the RMSE between 12 and 34%.

Furthermore, a procedure to decompose daily to hourly temperatures was also evaluated. It was found that the procedure, although originally developed using data from North American locations, produces reliable estimates of hourly temperature with a low MBE range that varied from −0.1 to −0.4°C and the RMSE range that varied between 1.6 and 3.7°C for three international locations. A review of models that decompose mean-daily irradiation to hourly data sets was also presented. It was found that this latter variable may be obtained with an accuracy figure of $\pm 20\ \mathrm{W/m^2}$ for over 50% of the time.

Finally, there are large body of existing data on the above parameters measured across the world in recent years. These data may be used for further validation of the proposed model for different geographic areas, climatic zones and seasons. The presently proposed statistical metrics may then be used to evaluate further accuracy enhancement that may thus be achieved.

ACKNOWLEDGEMENTS

The lead author (E.J.G.) is thankful to the Spanish Ministry of Education and to Granada University for providing financial assistance for this work. The authors also wish to thank Edinburgh Napier University, Transport Research Institute (TRI), for providing all necessary facilities.

REFERENCES

[1] Thornton PE, Running SW. An improved algorithm for estimating incident daily solar radiation from measurements of temperature, humidity, and precipitation. *Agric Meteorol* 1999;**93**:211–28.
[2] Rivisgton M, Matthews KB, Bunchan K. A comparison of methods for providing solar radiation data to crop models and decision support systems. In: *Proceedings of the Integrated assessment and decision support, 1st Biennial Meeting of International Environmental Modelling and Software Society*, **Vol. 3**, June 24–27 2002. 193–8.
[3] Angstrom A. Solar and terrestrial radiation. *QJR Meteorol Soc* 1924;**50**:121–5.
[4] Muneer T, Saluja G. A brief review of models for computing solar radiation on inclined surfaces. *Energy Convers Manage* 1985;**25**:443.
[5] Colliver D. In Parker B.F. (ed.) *Solar Energy in Agriculture. Energy in World Agriculture*. Elsevier, 1991.
[6] Muneer T. *Solar Radiation and Daylight Models,* 2nd edn. Elsevier, 2004.
[7] Campbell G. *An Introduction to Environmental Biophysics*. Springer, 1977.
[8] Bristow K, Campbell G. On the relationship between incoming solar radiation and daily maximum and minimum temperature. *Agric Meteorol* 1984;**31**:159–66.
[9] Hargreaves G, Samani Z. Estimating potential evapotraspiration. *J Irrig Drain Eng ASCE* 1982;**180**:225–30.

[10] Hargreaves G. Simplified coefficients for estimating monthly solar radiation in North America and Europe. Dept. Paper, Department of Biology and Irrigation Engineering, Utah State University. 1994.

[11] Annandale JG, Jovanovic NZ, Benade N, *et al*. Software for missing data error analysis of Penman–Monteith reference evapotraspiration. *Irrig Sci* 2002;**21**:57–67.

[12] Allen R. Evaluation of procedures for estimating mean monthly solar radiation from air temperature. *Report*. Food and Agriculture Organization of the United Nations (FAO). 1995.

[13] Allen R. Self-calibrating method for estimating solar radiation from air temperature. *J Hydrol Eng* 1997;**2**:56–67.

[14] Samani Z. Estimating solar radiation and evapotraspiration using minimum climatological data. *J Irrig Drain Eng ASCE* 2000;**126**:265–7.

[15] Meza F, Varas E. Estimation of mean monthly solar radiation as a function of temperature. *Agric Meteorol* 2000;**100**:231–41.

[16] Liu DL, Scott BJ. Estimation of solar radiation in Australia from rainfall and temperature observations. *Agric Meteorol* 2001;**106**:41–59.

[17] McCaskill MR. An efficient method for generation of full climatological records from daily rainfall. *Aust J Agrc Res* 1990;**41**:595–602.

[18] McCaskill MR. Prediction of solar radiation from rain information using regionally stable coefficients. *Agric Meteorol* 1990;**51**:247–55.

[19] Richardson CW. Weather simulation for crop management models. *Trans ASEA* 1985;**28**:1602–6.

[20] Hargreaves G, Riley J. Irrigation water requirement for Senegal River Basin. *J Irrig Drain Eng ASCE* 1985;**111**:265–75.

[21] De Jong R, Stewart DW. Estimating global solar radiation from common meteorological observations in Western Canada. *Can J Plant Sci* 1993;**73**:509–18.

[22] Hunt LA, Kuchar L, Swanton CJ. Estimation of solar radiation for use in crop modelling. *Agric Meteorol* 1998;**91**:293–300.

[23] Zhoy J, Wu Y, Yan G. General formula for estimation of monthly average daily global radiation in China. *Energy Convers Manage* 2005;**46**:257–68.

[24] Bandyopadhyay A, Bhadra A, Raghuwanshi NS, *et al*. Estimation of monthly solar radiation from measured air temperature extremes. *Agric Meteorol* 2008;**148**:1707–18.

[25] Swartman R, Ogunlade O. Solar radiation estimates from common parameters. In *Proceedings of Solar Energy Conference*, **Vol. 4,** 1967. 20–2.

[26] *ASHRAE Handbook of Fundamentals.* American Society of Heating, Refrigerating and Air-Conditioning Engineers, 2009.

[27] Liu B, Jordan R. The inter-relationship and characteristic distribution of direct, diffuse and total solar radiation. *Solar Energy* 1960;**4**:1.

[28] Whillier A. The determination of hourly values of total radiation from daily summations. *Archiv Meteorol Geophys Bioclimatol* 1956;**7**(Series B):197.

[29] Collares-Pereira M, Rabl A. The average distribution of solar radiation correlations between diffuse and hemispherical and between daily and hourly insolation values. *Solar Energy* 1979;**22**:155.

[30] Hawas M, Muneer T. Study of diffuse and global radiation characteristics in India. *Energy Convers Manage* 1984;**24**:143.

[31] Tham Y, Muneer T, Davison B. Estimation of hourly averaged solar irradiation: evaluation of models. *Build Serv Eng Res Technol* 2010;**31**:9.

[32] *ASHRAE Handbook of Fundamentals.* American Society of Heating, Refrigerating and Air-Conditioning Engineers, 1997.

[33] Muneer T, Abodahab N, Weir G, *et al*. *Windows in Buildings*. Elsevier, 2000.

[34] Hedrick R. Generation of hourly design-day weather data (RP-1363). ASHRAE Research Project, *Final Report*. 2009.

[35] Thevenard D. Updating the ASHRAE climatic data for design and standards (RP-1453). ASHRAE Research Project, *Final Report*. 2009.

[36] Coskun C, Oktay Z, Dincer I. A novel approach to cooling degree-hour calculation: an application for 58 cities in Turkey. In *5th International Ege Energy Symposium*, 27–30 June 2010, Pamukkale University.